WELDING RESEARCH

SUPPLEMENT TO THE *WELDING JOURNAL*, AUGUST 2003
Sponsored by the American Welding Society and the Welding Research Council

Experimental Study of Nugget Formation in Resistance Spot Welding

Nugget formation mechanism and its effect on the welding process parameters are observed by using a digital high-speed camera

BY Y. CHO AND S. RHEE

ABSTRACT. The nugget formation mechanism in resistance spot welding and its effect on the welding process parameters are examined by using a digital high-speed camera to visually monitor and observe the process of nugget formation. A modified half-section truncated-dome electrode and illumination system are introduced for the study, and the dynamic resistance, the main process parameter containing information on the nugget formation, is monitored and compared to the captured faying interface. In addition, the mechanism of nugget formation and the pulsing phenomenon, including heat generation and transfer, are examined based on the color changes of the faying interface and the development of a yellow-red heat zone. Variations of the lengths of the current path and the contact area of the faying interface are discussed together with equivalent resistivity across electrodes to consider the effect of the factors, which contribute to the increase and decrease of the dynamic resistance. Furthermore, the dominant factors contributing to the dynamic resistance change are also presented with high-speed photography.

Introduction

Resistance spot welding has been widely employed in sheet metal fabrication, particularly in the automotive industry. The nugget formation mechanism is very important for its influence on the strength and durability of the welded structure, and many researchers have investigated the formation mechanism of the nugget under various welding conditions and materials. In addition to the metallurgical approach examining the defects of the nugget or the effect of the chemical composition of the weld (Refs. 1, 2), the nugget in resistance spot welding has generally been observed through a macroscopic method using the destructive cross-sectional test of the weld (Refs. 3, 4). This nugget was typically observed after welding had been completed, thus making it difficult to measure the growth of the nugget. Numerical analyses are used to examine temperature distribution and corresponding nugget formation in the weld (Refs. 5–7). In the referred studies, the electrothermal response of the weld and the nugget diameter change were studied. Nevertheless, it is very difficult to analyze the heat distribution of the faying interface since the welding is electrically and thermomechanically coupled. In particular, the limitations of the simulation from a numerical analysis make it very difficult to consider the indentation of the weld. A number of researchers have suggested a method of visual observation of the nugget formation by using high-speed photography in order to effectively solve such problems. In research by Upthegrove et al. (Ref. 8), a specially machined electrode was used in a high-speed photographic analysis through which the nugget formation process of a coated sheet was explained and compared to the process on an uncoated sheet. In a followup study (Ref. 9), a more advanced lighting system was used to examine the effect of preheating and postheating on the nugget formation through high-speed cinematography. In that study, preheating current was used to induce nugget formation of a certain size to find a method to enhance the weld quality. Kim et al. (Ref. 10) used an infrared emission monitoring system to examine temperature change and heat transfer in the weld nugget as well as the parameters affecting nugget formation. Although the preceding studies observed the effect of the nugget formation phenomenon and current modification on weld quality, they did not take the correlation between nugget formation and the process parameters measured during the welding process into consideration.

The results of high-speed camera monitoring are used in this study to examine not only the formation and growth of the nugget but also the relationship between the process parameter and nugget formation, leading to a visual understanding of the physical meaning of dynamic resistance and the nugget formation mechanism. A number of researchers have experimented with the possibilities of the relationship between various process parameters and the growth of the weld nugget. In early studies (Refs. 11, 12), a cathode-ray oscilloscope was used to record the measured analog signal and calculate the dynamic resistance from the graph. Johnson et al. (Ref. 13) observed the electrode movement signal according to the weld expansion and examined the effect of the signal on weld quality, while Savage et al. (Ref. 14) and Dickinson et al. (Ref. 15) considered the electrode force, surface condition of the weld, welding current, welding voltage, dynamic resistance, and heat input energy from the resistance spot welding process to observe the nugget formation of the weld. In the latter study, the effect of nugget formation on dynamic resistance and the corresponding resistance patterns were observed, which ef-

KEY WORDS

Resistance Spot Welding
Nugget Formation
Process Parameter
High-Speed Camera
Dynamic Resistance

Y. CHO is Research Fellow, Department of Mechanical Engineering, The University of Michigan, Ann Arbor, Mich. S. RHEE is Professor, Department of Mechanical Engineering, Hanyang University, Seoul, Korea.

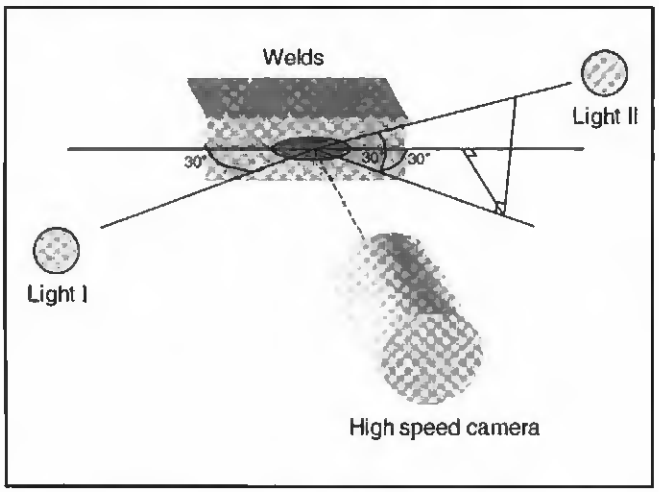

Fig. 1 — Schematic diagram indicating the placement of the camera and lighting system.

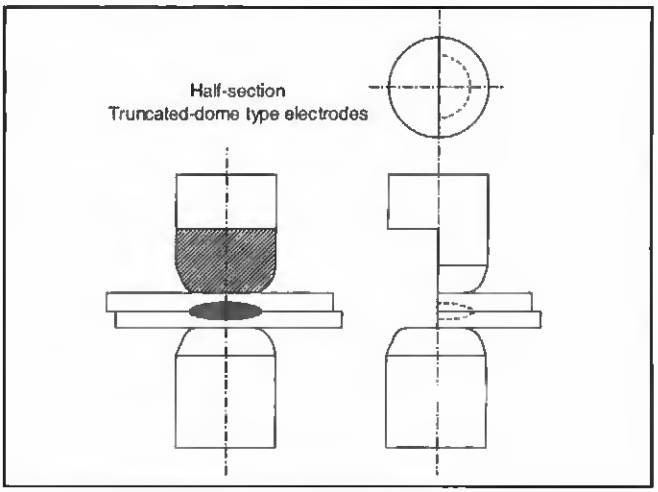

Fig. 2 — Half-section truncated-dome-type electrode and weld alignment.

fectively explained the change of the dynamic resistance patterns according to the stages of nugget formation, including the collapse of contact resistance, increase in faying surface temperature, melting, and plastic deformation. With the advances in measuring devices and technology, various dynamic parameter-monitoring systems in addition to dynamic resistance are suggested (Ref. 16). In recent studies, a new controller-based dynamic resistance monitoring system was developed for in-process system environments such as automobile manufacturing lines (Refs. 17, 18). Based on the above surveys, the relation between the mechanism of nugget formation and the corresponding process parameter was observed with a digital high-speed camera monitoring system.

Experimental Procedure

The experimental procedure was divided into three stages: welding process, nugget growth monitoring, and process parameter monitoring. Welding was performed on a 75-kVA pneumatically operated resistance welding machine; the nugget formation of the welding zone was monitored with a digital high-speed camera and a specially designed electrode tip and illumination system. Dynamic resistance was determined as the process parameter due to its close correlation to the growth of the weld nugget. The changes in dynamic resistance were observed throughout the welding process.

Nugget Formation Monitoring

The experimental setup for the digital high-speed camera is shown in Fig. 1. Kodak Motion Corder Analyzer SR-Ultra/c was used to monitor the nugget formation at high speed. The system was comprised of a processor, power supply, camera, viewfinder, and lighting sources. A resolution of 256 × 240 pixels was used in order to capture the nugget formation. The camera system consisted of an adapter plate, camera head, tripod, and lens. A standard C-mount lens adapter and SPACECOM CCTV lens model H16X8M-II, which has a focal length of 8–48 mm, zoom ratio of 16x, and aperture (F) of 1:1.0 were used. Two sets of No. 1, No. 2, and No. 3 Kenko close-up lenses were used in order to obtain an enlarged image of the nugget with a UV filter protecting the main lens from expelled molten material. The choice of illumination system, such as type, intensity, and location, is very important when using a high-speed camera, and thus two 40-W halogen lamps, which are shown in Fig. 1, were used to illuminate the welding zone.

A specially designed electrode was used in order to monitor the process of nugget growth as shown in Fig. 2. A 16-mm-diameter dome-type electrode with a 6-mm-diameter tip end made with copper alloy of RWMA class II chrome cut in half was used as an upper electrode of the welding machine. Although the heat transfer rates of the upper and lower electrodes were not exactly the same and the physical constraints of this experiment were not those of ordinary welding conditions, the heat generation and nugget growth were expected not to be significantly different from those of a normal weld (Ref. 9).

A 1.4-mm-thick uncoated steel plate of the type used in the automotive industry was cut into 20 × 40-mm pieces. Using clips, the two sheets were aligned with the front face and then welded. The front face of each specimen pair was ground flat with a file and finished with a 600x abrasive. The final finishing treatment was applied only vertically in consideration of the angle of the light source in order to effectively diffuse reflection from the light source in Fig. 1.

Dynamic Resistance Monitoring

In resistance spot welding, there is a direct correlation between the nugget formation and the various welding variables, including the electrode force, welding current, welding time, and material characteristics. Among the welding parameters that can be monitored, dynamic resistance, in particular, is closely related to weld nugget formation (Refs. 14–16). In general, dynamic resistance is measured in the secondary circuit of the welding machine and utilized in many different methods. Recent studies, however, have led to the development of a primary circuit monitoring system, which overcomes the disadvantage of the secondary circuit monitoring system with its applicability to in-process system environments (Refs. 17, 18). This system was implemented in this study where dynamic resistance, which is monitored in the primary circuit of the welding machine, was used to observe the relation between nugget formation and the process parameters.

Welding Condition

A 1.4-mm-thick sheet of uncoated steel with the material properties shown in Table 1 was used for welding. The electrode force in this study was reduced to half (1.96 kN) as an equivalent force to normal conditions since the force of the full-section electrode on the weld is twice as large as the force of the half-section electrode. As for the current source, the heat generated by the full-section electrode H_f is proportional to the current

square, as shown in Equation 1.

$$H_f = I^2 R_f t \quad (1)$$

where I is the welding current, R_f is the resistance of the weld with the full-section electrode and t is time. The resistance of the weld R is increased to twice the value as the contact area reduces to half the size in Equation 2.

$$R = \rho \frac{l}{A} \quad (2)$$

where p is the electrical resistivity, l is the length of the conductor, and A is the contact area. In order to obtain an equal welding performance with a half-section electrode as with a full-section electrode, half the amount of heat $H_f/2$ is needed and this requires the current to be decreased by half. A comparison between the welding condition with the full-section electrode and the half-section electrode is shown in Table 2.

Results and Discussions

In this section, the nugget formation was observed with the captured frames. In addition, examination of the effect of the nugget formation on the dynamic resistance, which is a process parameter, was considered.

Nugget Formation

The electrode force and welding time were fixed at 1.96 kN and 15 cycles, respectively. The current varied throughout the welding from 5.5 to 8 kA, and the welding process was recorded at 1000 frames/second, from which eight or nine pictures were obtained out of each half cycle. Figure 3 shows the typical nugget formation of the experiments, using a 6.5-kA welding current. The vertical cross section of the weld, at the moment the largest nugget is developed during each upper-half cycle, is shown along the welding cycle. In the beginning stages of welding, fumes — alleged to be from residue left on the weld surface — are observed. At the 4th cycle of welding, the front face is darkened in color due to the heat generated at the faying interface between the two sheets. The darkening phenomenon initiates as a circular shape, which expands into a square-like shape after the 6th cycle. The shape of the darkened area provides valuable information about the initial heat generation and the transfer process. The darkened area began at the center and extended to the width of the tip end until it reached the electrode-sheet contact face at the 8th cycle. A yellow-red heat zone directly related to the formation of the welded nugget was generated at the 9th cycle and the total thickness of the two sheets noticeably decreased after formation of the yellow-red heat zone, leading to a hypothesis that the phenomenon is based upon the solid-state material between the electrodes, which sustain the electrode force, not existing any longer by heating; thus causing plastic deformation. The growth pattern of the nugget throughout the 10th and 11th cycles showed the validity of this explanation.

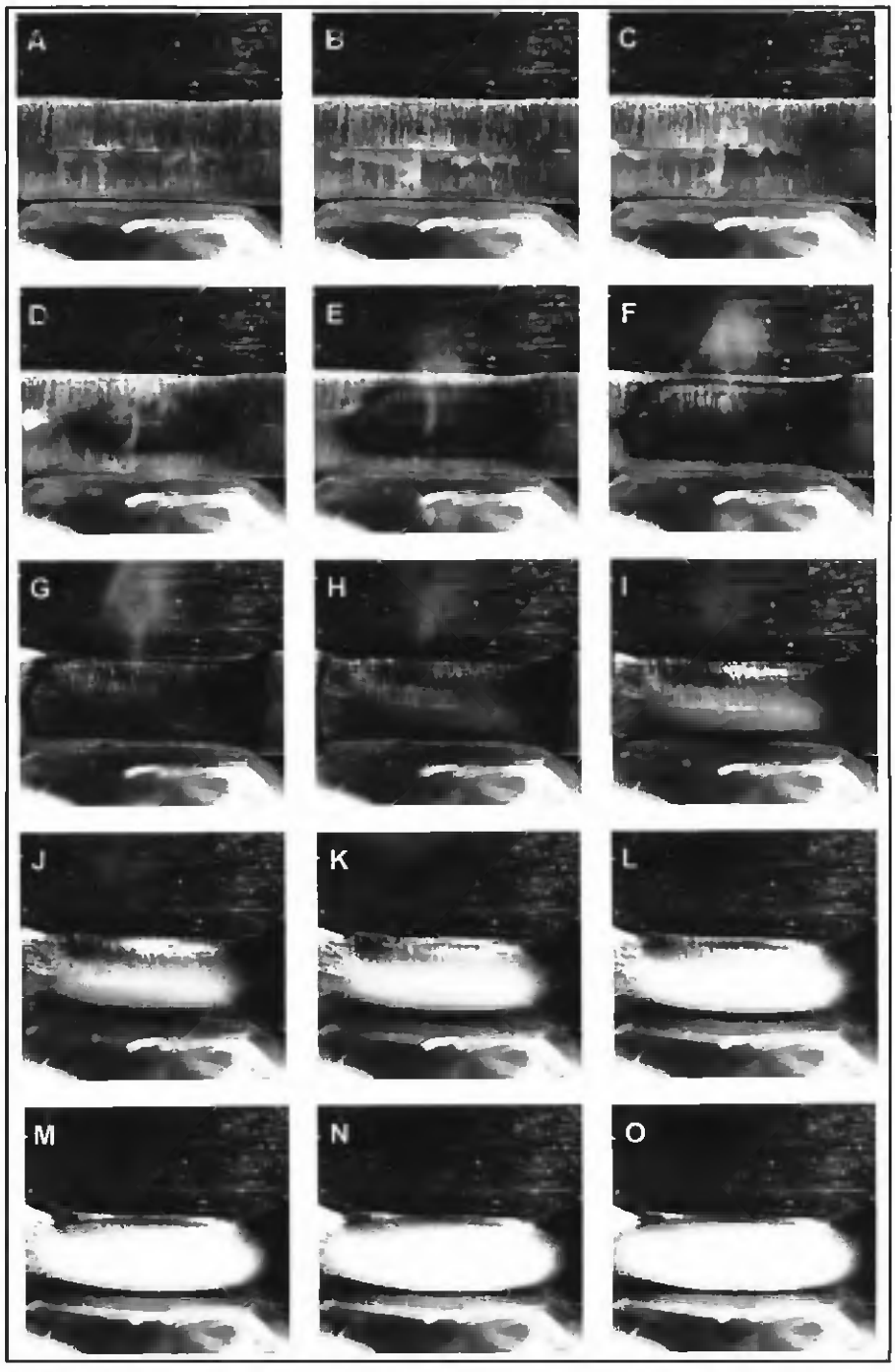

Fig. 3 — Photographs of nugget formation monitored by the digital high-speed camera.

A 60-Hz alternating current was used as the welding current, causing a pulsing phenomenon during welding (Refs. 8, 19), and this phenomenon can be seen upon the generation of the yellow-red zone. In order to visualize the pulsing phenomenon, captured images were transformed into black and white images by the image processing technique. An examination of the image shown in Fig. 3K shows the yellow-red zone of the nugget has been changed into a contour, and the major and minor axes of the nugget size pulsing with the alternating current were taken into consideration by measuring the width and height of the con-

Table 1 — Material Properties of Base Material, Bare Steel 1.4 mm

Chemical Compositions (wt-%)						Mechanical Properties (kgf/mm^2)	
C	Si	Mn	P	S	Fe	YP	TS
0.0030	0.002	0.04	0.009	0.008	Bal.	17.0	30.6

Table 2 — Comparison of Welding Condition; Full-Section Electrode vs. Half-Section Electrode

	Thickness (mm)	Electrode Force (kN)	Welding Time (cycle)	Welding Current (kA)
Regular electrode	1.4	3.92	15	14
Half-section electrode	1.4	1.96	15	7

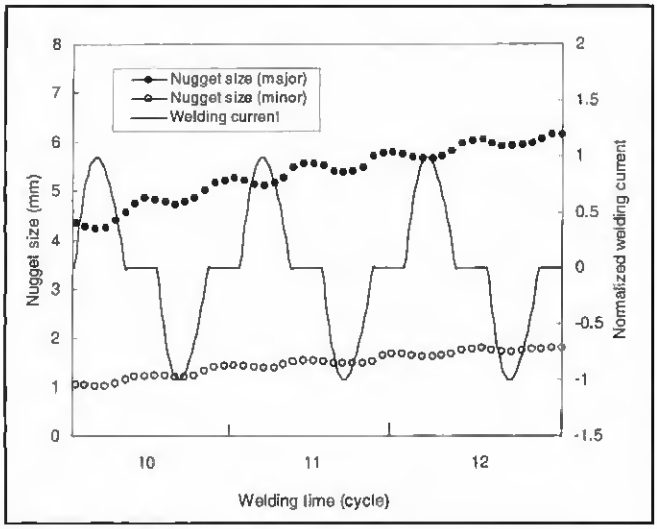

Fig. 4 — Pulsing phenomenon coincident with the monitored welding current.

tour. As an example of the pulsing behavior, the normalized current waveform monitored by a sampling rate of 6 kHz and the corresponding nugget sizes are illustrated in Fig. 4. As predicted in the preceding analytical studies (Ref. 19), the nugget formed in accordance with the alternating pattern. The nugget expanded in all directions with an oscillation of twice the frequency of the welding current according to the progression of the cycle. The oscillation lagged behind the driving current because of the heat capacity and thermal conductance of the sheet. The variations around the average value tended to be ±7% in the major axis and ±9% in the minor axis at the beginning of the 10th cycle. As the size was increased and saturated, the variations became approximately ±2% of the average value in both axes at the end of the 12th cycle.

Influencing Factors on Dynamic Resistance

The dynamic resistance pattern monitored during the welding cycle and the corresponding series of pictures are presented. Through the analysis of these pictures, the effect of the nugget formation process on the dynamic resistance was observed.

Figure 5 shows the series of pictures obtained in the previous section, which were cut and rearranged only in the center of the nugget image along the welding cycle. The corresponding dynamic resistance patterns of the five different welding conditions are given in Fig. 6. Figures 7 and 8 show the variations of the lengths of the current path and the contact area of the faying interface, which are presented by measuring the total thickness of the weld and the size of the corona bond, based on the monitored pictures. These results were used to calculate the variation of equivalent resistivity across electrodes indirectly using Equation 2. The values of the equivalent resistivity were normalized to a maximum value of 100% in Fig. 9.

When welding was performed with a current of 5.5 kA — considered a relatively low current — a decrease in resistance during the first two cycles and a local minimum at the 2nd cycle called alpha-minimum (Ref. 15) was observed. This minimum value is caused by the competition between the collapse of the faying surface asperities causing resistance to decrease and increasing temperature results in increasing resistivity providing an opposite effect. From the next cycle, a continuous increase of the dynamic resistance caused by a temperature rise in the weld was observed. The increase rate of dynamic resistance continued to slow with the progression of the welding cycle until the 13th cycle. The dynamic resistance at that point ceased to increase with the generation of the yellow-red heat zone in Fig. 6A. The indentation of the weld, which is the difference between initial total thickness of the welds and measured thickness at each cycle, slowly began to take form at the 9th cycle. After the generation of the indentation, the factor contributing to the increase of the dynamic resistance, such as an increase in bulk resistivity of the substrate resulting from increasing temperature as it heats up, outweighed the factors contributing to the decrease in dynamic resistance. Those factors included a shortening of the path for current flow resulting from some mechanical collapse caused by increased softening and an increase in area due to plastic flow of the hot metal available for current flow, thus causing a slight increase in the dynamic resistance (Refs. 14–16, 20). In conclusion, the two factors become equal after the 13th to 15th cycles and the dynamic resistance ceased to increase. When the welding current was 6.0 kA, an indentation began to form at the 6th cycle before the yellow-red heat zone was generated at the 12th cycle. Similar to 5.5 kA, the decrease rate of the thickness in Fig. 7 was approximately 0.028 mm/cycle, and the effect of the factors contributing to the decrease and increase of the dynamic resistance, in addition, were considered nearly equal as the dynamic resistance does not show a significant decrease during the interval where the indentation is being formed. The increase rates of the corona bond were 0.31 mm/cycle and 0.33 mm/cycle for the 5.5 and 6.0 kA condition, respectively. The change rates of the equivalent resistivity, furthermore, showed 6.70%/cycle and 6.47%/cycle, respectively.

When the welding current was 6.5 kA — a relatively optimal welding condition — more than 0.2 mm of indentation was formed before the yellow-red zone was generated at the 9th cycle, as in Figs. 5C and 7. After the 9th cycle, unlike the increase rate of the corona bond (0.30 mm/cycle) and the change rates of the equivalent resistivity (6.26%/cycle) — almost identical values to the two previous low current conditions — the decrease rate of thickness showed 0.044 mm/cycle, which was slightly less than twice as high as the two previous conditions. In that case, the decrease in the length of the current path dominantly affects the change in the dynamic resistance, and thus a decrease in dynamic resistance (1.14 μΩ/cycle), can be seen after the 9th cycle.

It can also be seen in Fig. 5C that the nugget formed after three or four cycles of the beta peak (Refs. 15, 20), which was defined by the result of the competing effects of increasing bulk resistivity with temperature and decreasing interface resistance.

When higher currents of 7.5 and 8.0 kA were applied, thus generating more heat, the dynamic resistance increased more rapidly. The beta peak was observed in the 5th cycle and the yellow-red heat zone in the next cycle on the 7.5-kA condition. During the five cycles after beta peak, a rapid decrease of dynamic resistance (3.64 μΩ/cycle) was shown with the increase rate of the corona bond of 0.67 mm/cycle and the decrease rate of thickness of 0.11 mm/cycle resulting in resistance decrease, which is higher than twice the 6.5-kA condition. The change rate of the equivalent resistivity showed the value of 12.01%/cycle as the factor causing the resistance to increase, which is slightly less than twice as high as to the value of the 6.5-kA condition. After the 11th cycle, the equivalent resistivity tended to saturate in time and become constant, and the dynamic resistance still uniformly decreased (0.96 μΩ/cycle) during this period, not due to the change of the equivalent resistivity (0.11%/cycle) but mainly because of the change in the current path (0.03 mm/cycle), possibly for the fact that the weld nugget was fully grown after the 11th cycle and the temperature began to stabilize. In the case of the 8.0-kA condition, the yellow-red heat zone was observed right after the beta peak in Fig. 5E, and the most rapid changes occurred in the period between the 4th and 6th cycles such as 6.32 μΩ/cycle in dynamic resistance, 0.21 mm/cycle in thickness, 1.20 mm/cycle in the corona bond, and 25.45%/cycle in equivalent resistivity. During the period between the 7th and 9th cycles, the increase rate of the corona bond and the decrease rate of thickness became smaller in conjunction with the decrease in dynamic resistance, and the aforementioned changes became less apparent after the 10th cycle. Once the equivalent resistivity in Fig. 9 was saturated after the 7th cycle, the dynamic resistance tended to be affected by the change in the area and length available for current flow rather than temperature.

Based on the above discussion, it becomes possible to visually understand the physical implications of the changes or patterns of the process parameters. It is also confirmed that the nugget formation has a direct effect on the change in the dynamic resistance. These results show that the information on the nugget can be obtained easily if the pattern or changes in the process parameters are examined by online monitoring during the welding process. This, in addition, makes it possible to effectively evaluate the quality of the welds in real time.

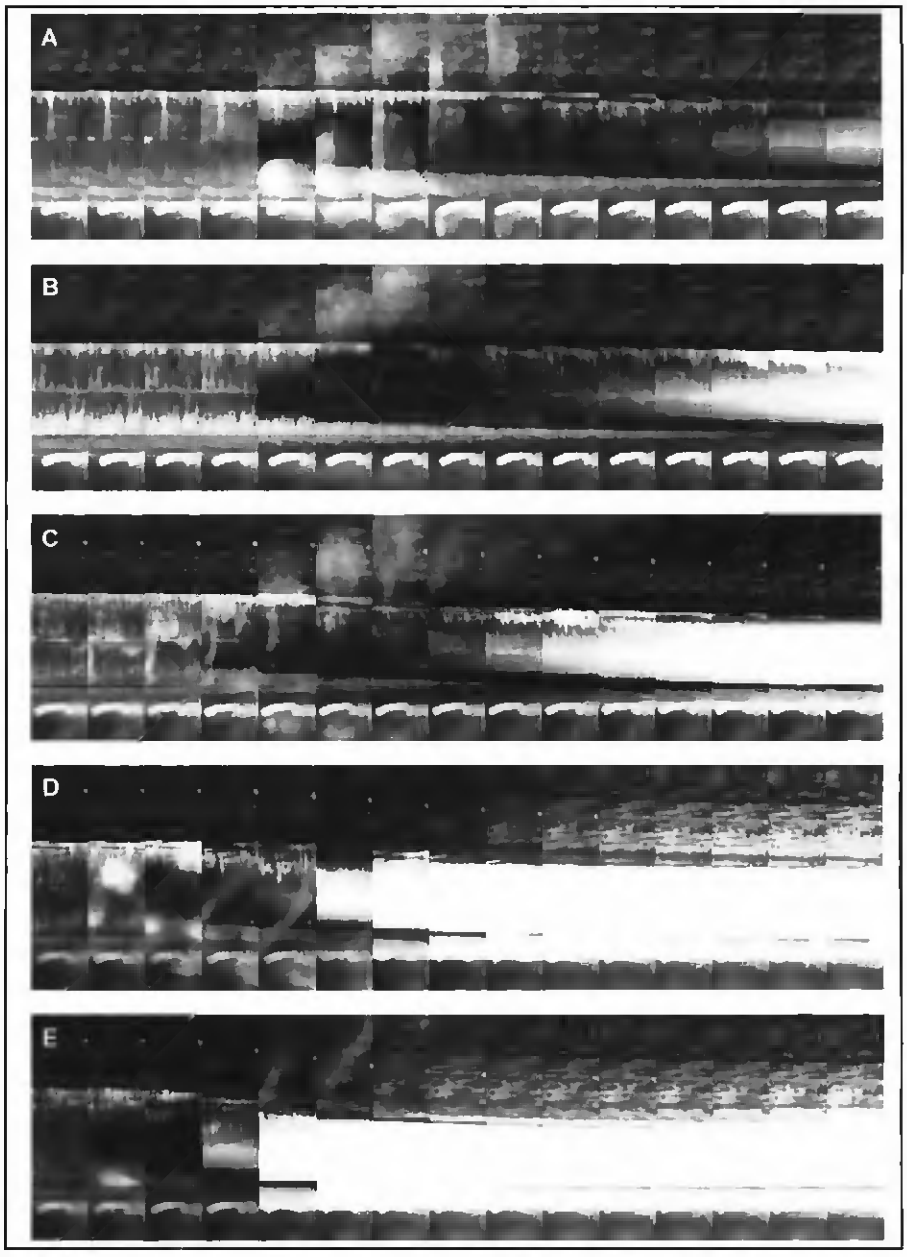

Fig. 5 — Time series of nugget formation with various welding conditions.

Conclusion

The nugget formation mechanism in resistance spot welding and its relation to the process parameters were examined using a digital high-speed camera. Using the half-section truncated-dome-type electrode and illumination system, the formation and growth of the nugget were monitored at 1000 frames/second, with a resolution of 256 × 240 pixels. The results were compared to the changes in dynamic resistance. Based on the darkening phenomenon of the front face of the welded zone, the shape of the heat generation occurring in the primary stages of welding was observed. The initial heat appeared in a small rounded shape on the faying interface and expanded into a square shape, which extended to the width of the tip end on the electrode-sheet contact face. As welding progressed, the yellow-red heat zone directly related to the nugget was generated at the center of the weld. The nugget expanded in all directions and oscillated with twice the frequency of the welding current along with a time lag according to the progression of the cycle. The nugget size tended to be saturated in a certain size with the decrease in oscilla-

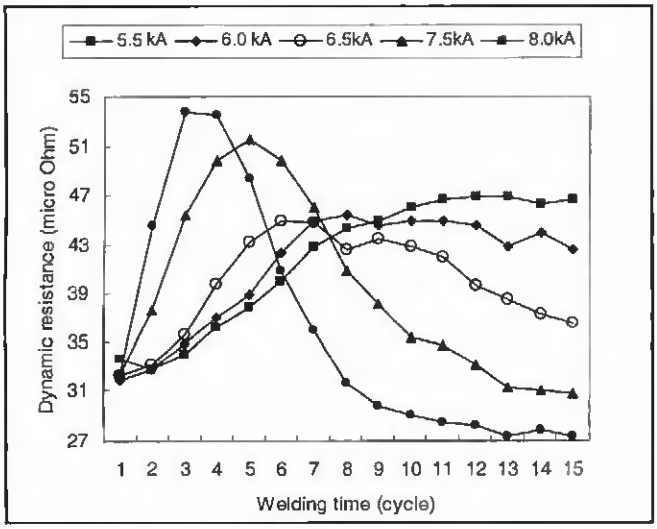

Fig. 6 — Comparison of dynamic resistance for five different welding currents.

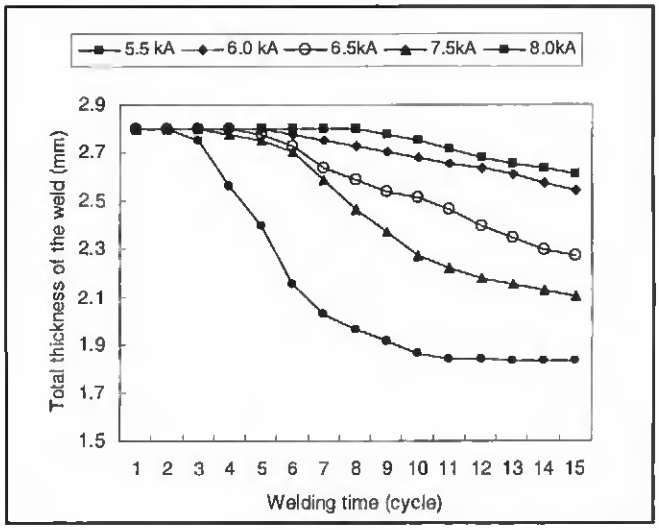

Fig. 7 — Comparison of total thickness of the weld for five different welding currents.

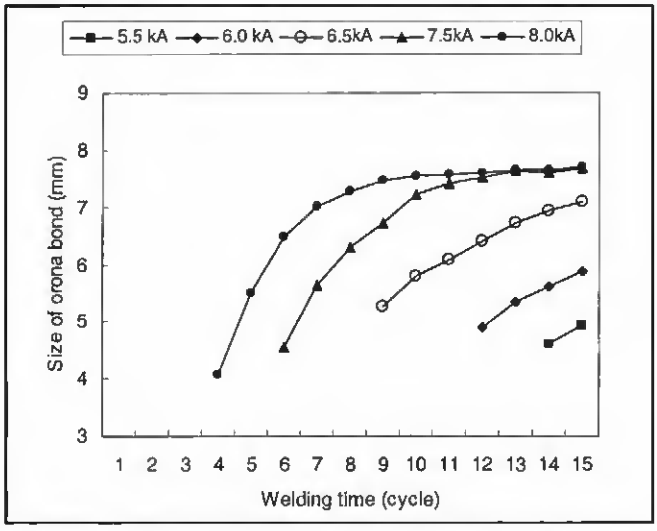

Fig. 8 — Comparison of the size of the corona bond for five different welding currents.

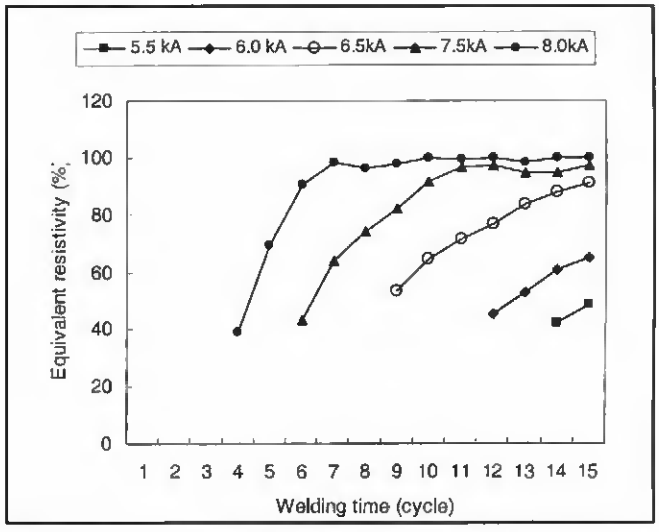

Fig. 9 — Comparison of the equivalent resistivity for five different welding currents.

tion. The dynamic resistance is discussed with the total thickness of the weld, the size of corona bond and equivalent resistivity of the weld, which are obtained from the pictures of the nugget formation to conclude the following results. The dynamic resistance reached equilibrium during the low welding current at around 0.028 mm/cycle of the decrease rate of thickness, 0.33 mm/cycle of the increase rate of corona bond, and 6.47%/cycle of the increase rate of equivalent resistivity. When a proper welding current was applied, the yellow-red heat zone was formed after three or four cycles of the beta peak, and the decrease in the length of the current path dominantly affected the change in dynamic resistance after the formation of that zone. At the high current condition, the equivalent resistivity tended to saturate in time and became constant due to the temperature beginning to stabilize. The dynamic resistance was affected by the change of the area and length available for current flow rather than temperature after the saturation. The relationship between the dynamic resistance and the nugget formation, therefore, was visually explained, and the implications of the pattern and change of the process parameter were examined.

Acknowledgments

This work has been supported by a grant from the Brain Korea 21 Project and the Critical Technology 21 Project of the Ministry of Science and Technology, Korea.

References

1. Sawhill, J. M., Jr., and Baker, J. C. 1980. Spot weldability of high-strength sheet steels. *Welding Journal* 59(1): 19-s to 30-s.

2. Gould, J. E. 1994. Modeling primary dendrite arm spacings in resistance spot welds, Part II — Experimental studies. *Welding Journal* 73(5): 91-s to 100-s.

3. Cho, H. S., and Cho, Y. J. 1989. A study of the thermal behavior in resistance spot welding. *Welding Journal* 68(6): 236-s to 244-s.

4. Gould, J. E. 1987. An examination of nugget development during spot welding using both experimental and analytic techniques. *Welding Journal* 66(1): 1-s to 10-s.

5. Nied, A. 1984. The finite element modeling of the resistance spot welding process. *Welding Journal* 63(4): 123-s to 132-s.

6. Vogler, M. M. B. 1993. Investigation of Resistance Spot Weld Formation. Ph.D. diss., Stanford University.

7. Na, S. J., and Park, S. W. 1996. A theoretical study on electrical and thermal response in resistance spot welding. *Welding Journal* 75(9): 233-s to 241-s.

8. Upthegrove, W. R., and Key, J. F. 1972. A high speed photographic analysis of spot welding

galvanized steel. *Welding Journal* 51(5): 233-s to 244-s.

9. Lane, C. T., Sorensen, C. D., Hunter, G. B., Gedeon, S. A., and Eagar, T. W. 1987. Cinematography of resistance spot welding of galvanized steel sheet. *Welding Journal* 66(9): 260-s to 265-s.

10. Kim, E. W., and Eagar, T. W. 1989. Measurement of transient temperature response during resistance spot welding, *Welding Journal* 68(8): 303-s to 312-s.

11. Tylecote, R. F. 1941. Spot welding, part II: Contact resistance. *Welding Journal* 20(12): 591-s to 602-s.

12. Roberts, W. L. 1951. Resistance variations during spot welding. *Welding Journal* 30(11): 1004-s to 1019-s.

13. Johnson, K. I., and Needham, J. C. 1972. New design of resistance spot welding machine for quality control. *Welding Journal* 51(3): 1-s to 8-s.

14. Savage, W. F., Nippes, E. F., and Wassell, F. A. 1978. Dynamic contact resistance of series spot welds. *Welding Journal* 57(2): 43-s to 50-s.

15. Dickinson, D. W., Franklin, J. E., and Stanya, A. 1980. Characterization of spot welding behavior by dynamic electrical parameter monitoring. *Welding Journal* 59(6): 170-s to 176-s.

16. Gedeon, S. A., Sorensen, C. D., Ulrich, K. T., and Eagar, T. W. 1987. Measurement of dynamic electrical and mechanical properties of resistance spot welds. *Welding Journal* 66(12): 378-s to 385-s.

17. Cho, Y., and Rhee, S. 2002. Primary circuit dynamic resistance monitoring and its application to quality estimation during resistance spot welding. *Welding Journal* 81(6): 104-s to 111-s.

18. Cho, Y., and Rhee, S. 2000. New technology for measuring dynamic resistance and estimating strength in resistance spot welding, *Measurement Science and Technology* 11(8): 1173–1178.

19. Archer, G. R. 1960. Calculations for temperature response in spot welds. *Welding Journal* 39(8): 327-s to 330-s.

20. Kaiser, J. G., Dunn, G. J., and Eagar, T. W. 1982. The effect of electrical resistance on nugget formation during spot welding. *Welding Journal* 61(6): 167-s to 174-s.